

# Relating Topological Determinants of Complex Networks to Their Spectral Properties: Structural and Dynamical Effects

Claudio Castellano<sup>1</sup> and Romualdo Pastor-Satorras<sup>2, \*</sup>

<sup>1</sup>*Istituto dei Sistemi Complessi (ISC-CNR), Via dei Taurini 19, I-00185 Roma, Italy*

<sup>2</sup>*Departament de Física, Universitat Politècnica de Catalunya, Campus Nord B4, 08034 Barcelona, Spain*

The largest eigenvalue of a network's adjacency matrix and its associated principal eigenvector are key elements for determining the topological structure and the properties of dynamical processes mediated by it. We present a physically grounded expression relating the value of the largest eigenvalue of a given network to the largest eigenvalue of two network subgraphs, considered as isolated: The hub with its immediate neighbors and the densely connected set of nodes with maximum  $K$ -core index. We validate this formula showing that it predicts with good accuracy the largest eigenvalue of a large set of synthetic and real-world topologies. We also present evidence of the consequences of these findings for broad classes of dynamics taking place on the networks. As a byproduct, we reveal that the spectral properties of heterogeneous networks built according to the linear preferential attachment model are qualitatively different from those of their static counterparts.

arXiv:1703.10438v2 [physics.soc-ph] 30 Oct 2017

---

\* Corresponding author: romualdo.pastor@upc.edu

## I. INTRODUCTION

The spectral properties of complex topologies [1] play a crucial role in our understanding of the structure and function of real networked systems. Various matrices can be constructed for any given network, their spectral properties accounting for different topological or functional features. Thus, for example, the Laplacian matrix is related to diffusive and random walk dynamics on networks [2], the modularity matrix plays a role in community identification on networks [3], while the non-backtracking or Hashimoto matrix governs percolation [4]. Among all matrices associated to networks, the simplest and possibly most studied is the adjacency matrix  $A_{ij}$ , taking the value 1 whenever nodes  $i$  and  $j$  are connected, and zero otherwise. Particular interest in this case is placed on the study of the principal eigenvector  $\{f_i\}$  (PEV), defined as the eigenvector of the adjacency matrix with the largest eigenvalue  $\Lambda_M$  (LEV). This interest is twofold. On the one hand, the PEV is one of the fundamental measures of node importance or centrality [5]. The centrality of a node can be defined based on the number of other different vertices that can be reached from it, or the role it plays in connecting together different parts of the network. From a more sociological point of view, a node is central if it is connected to other central nodes. From this definition arises the notion of eigenvector centrality of a node [6], that coincides with the corresponding component of the PEV. On the other hand, the LEV plays a pivotal role in the behavior of many dynamical systems on complex networks, such as epidemic spreading [7], synchronization of weakly coupled oscillators [8], weighted percolation on directed networks [9], models of genetic control [10], or the dynamics of excitable elements [11]. In this kind of dynamical processes, the LEV is related, through different analytical techniques, to the critical point at which a transition between different phases takes place: In terms of some generic control parameter  $\lambda$ , a critical point  $\lambda_c$  is found to be in general inversely proportional to the LEV  $\Lambda_M$ .

The possibility to know the position of such transition points in terms of simple network topological properties is of great importance, as it allows to predict the system macroscopic behavior or optimize the network to control processes on it. This has triggered an intense activity [12–15], particularly in the case of networks with heterogeneous topology, such as power-law distributed networks with a degree distribution of the form  $P(q) \sim q^{-\gamma}$  [16]. Among these efforts, in their seminal work [17], Chung, Lu and Vu (CLV) have rigorously proven, for a model with power-law degree distribution, that the LEV can be expressed in terms of the maximum degree  $q_{\max}$  present in the network and the first two moments of the degree distribution. This is a remarkable achievement, as it allows to draw predictions in the analysis of dynamics on networks.

Here we show that while the CLV theory provides in some cases an excellent approximation to the LEV, specially in the case of random uncorrelated networks, it can fail considerably in other cases. In order to provide better estimates, we reinterpret the CLV result in terms of the competition among different subgraphs in the networks. This insight leads us to the formulation of a modified form of the CLV theory, that captures the behavior of the LEV more generally, including the case of real correlated networks, and asymptotically reduces to the CLV form in the case of random uncorrelated networks. We show that our generalized expression perfectly predicts the LEV for linear preferential attachment growing networks (for which the original CLV form fails) and provides an excellent approximation for the LEV of real-world networks. Finally, we show that our modified expression predicts reliably the critical point of dynamical processes on a large set of synthetic and real-world networks, with no exception.

The paper is organized as follows: In Sec. II we review the original expression for the largest eigenvalue from Ref. [17], and show how it can lead to large errors in real correlated networks. In Sec. III we present physical arguments substantiating a new generalized expression for the largest eigenvalue, whose validity is checked against a large set of real networks. In Sec. IV we discuss in detail the case of growing linear preferential attachment networks, which turn out to be a remarkable benchmark for the plausibility of our new generalized expression. We discuss the effects of our prediction in the estimation of the critical point in epidemics and synchronization dynamics in Sec. V. Finally, we present our conclusions and future avenues of work in Sec. VI. Several appendices provide details and additional information.

## II. THE CHUNG-LU-VU FORMULA FOR THE LARGEST EIGENVALUE

In Ref. [17], the authors consider a class of network models with given expected degree distribution. That is, starting from a predefined degree distribution  $P(q)$ , one generates expected degrees  $\tilde{q}_i$  for each node, drawn from  $P(q)$ , and creates an actual network by joining every pair of nodes  $i$  and  $j$  with probability  $\tilde{q}_i \tilde{q}_j / \sum_r \tilde{q}_r$ . The resulting network has a degree distribution with the same functional form as the imposed  $P(q)$  and lacks degree correlations, since the condition  $\tilde{q}_i^2 < \sum_r \tilde{q}_r$  is imposed in the construction [17, 18]. This algorithm is a variation of the classical configuration model [14], cast in terms of a hidden variables model [19]. For this model network, and any arbitrary degree distribution, the authors in Ref. [17] rigorously prove that the largest eigenvalue of the corresponding adjacency matrix takes the form (see also [20])

$$\Lambda_M = \begin{cases} a_1 \sqrt{q_{\max}} & \text{if } \sqrt{q_{\max}} > \frac{\langle q^2 \rangle}{\langle q \rangle} \ln^2(N) \\ a_2 \frac{\langle q^2 \rangle}{\langle q \rangle} & \text{if } \frac{\langle q^2 \rangle}{\langle q \rangle} > \sqrt{q_{\max}} \ln(N) \end{cases}, \quad (1)$$

where  $N$  is the network size,  $q_{\max}$  is the maximum degree in the networks, and  $a_i$  are constants of order 1. In the case of scale-free networks, the maximum degree is a growing function of  $N$ , that for uncorrelated networks [21] takes the value  $q_{\max} \sim N^{1/2}$  for

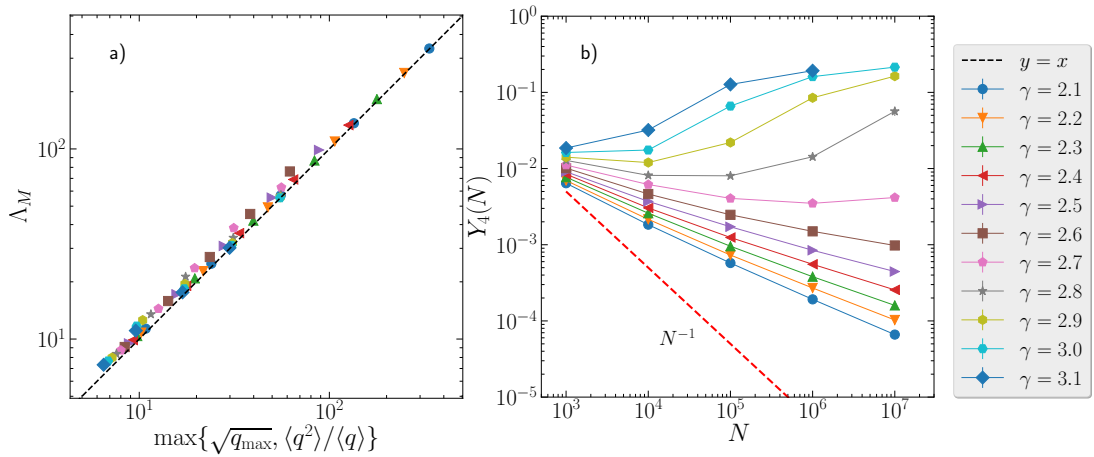


FIG. 1. (a) Largest eigenvalue  $\Lambda_M$  as a function of  $\max\{\sqrt{q_{\max}}, \langle q^2 \rangle / \langle q \rangle\}$  in uncorrelated power-law UCM networks with different degree exponent  $\gamma$  and network size  $N$ . (b) Inverse participation ratio  $Y_4(N)$  as a function of  $N$  in uncorrelated power-law UCM networks with different degree exponent  $\gamma$ . Each point in both graphs corresponds to an average over 100 independent network realization. Error bars are smaller than symbol sizes. Networks have a minimum degree  $m = 3$ .

$\gamma \leq 3$  and  $q_{\max} \sim N^{1/(\gamma-1)}$  for  $\gamma > 3$  [18]. The algebraic increase of  $q_{\max}$  allows to disregard the logarithmic terms in Eq. (1) in the limite of infinite size networks, leading to the simpler expression [22]

$$\Lambda_M \approx \max\{\sqrt{q_{\max}}, \langle q^2 \rangle / \langle q \rangle\}, \quad (2)$$

valid for any value of  $\gamma$ . For power law distributed networks, the second moment of the degree distribution scales as  $\langle q^2 \rangle \sim q_{\max}^{3-\gamma}$  for  $\gamma \leq 3$  and  $\langle q^2 \rangle \sim \text{const.}$  for  $\gamma > 3$ . Combining this result with the expression for the maximum degree, we can write the more explicit result

$$\Lambda_M \approx \begin{cases} \sqrt{q_{\max}} & \text{if } \gamma > 5/2 \\ \langle q^2 \rangle / \langle q \rangle & \text{if } \gamma < 5/2 \end{cases}. \quad (3)$$

It is important to remark that while Eq. (2) holds for asymptotically large networks, its applicability to networks of finite (yet huge) size should not be taken for granted. The exact Eq. (1) does not provide predictions for a wide (size-dependent) range of values of the ratio  $\langle q^2 \rangle / [\langle q \rangle \sqrt{q_{\max}}]$ . As shown in Appendix A, uncorrelated power-law distributed networks fall within this range for the span of network sizes usually considered in computer simulations, so that Eq. (1) does not provide predictions about any uncorrelated power-law networks that can be numerically simulated. Nevertheless, Eq. (2), which is a nonrigorous generalization of the exact Eq. (1), turns out to be very accurate for random uncorrelated static networks even of small size. Indeed, in Fig. 1a we present a scatter plot of  $\Lambda_M$  computed using the power iteration method [23] in random uncorrelated power-law networks generated with the uncorrelated configuration model (UCM) [24], for different values of the degree exponent  $\gamma$  and network size  $N$ , as a function of the numerically estimated value of  $\max\{\sqrt{q_{\max}}, \langle q^2 \rangle / \langle q \rangle\}$ . The agreement with Eq. (2) (in the following denoted as CLV theory) is almost perfect, with only very small deviations for the smallest network sizes.

In order to test the generality of CLV theory beyond uncorrelated networks, we have also considered a large set of 109 real-world networks (the same considered in Ref. [25], see this reference for network details), of widely different origin, size and topological features. In Fig 2a we plot the LEV of these networks as a function of the numerically estimated quantity  $\max\{\sqrt{q_{\max}}, \langle q^2 \rangle / \langle q \rangle\}$ . The result is quite clear: While in some cases the CLV prediction works well, in others it provides a overestimation of the actual value of the LEV that can be larger than one order of magnitude. This discrepancy is particularly strong in the case of the Zhishi, DBpedia, and Petster, cats networks, but it is considerable in a large number of other cases.

### III. GENERALIZED FORMULA FOR THE LARGEST EIGENVALUE

We can understand the origin of the violations of the CLV formula observed in Fig. 2a and provide an improved version, by reconsidering the observations made in Refs. [26, 27]. In these works it is shown that the two types of scaling of the LEV in the CLV formula for uncorrelated networks (either proportional to  $\langle q^2 \rangle / \langle q \rangle$  or to  $\sqrt{q_{\max}}$ ) are the manifestation of the two alternative ways in which the PEV can become localized in the network (see Appendix B). For  $\gamma > 5/2$  the PEV is localized around the node

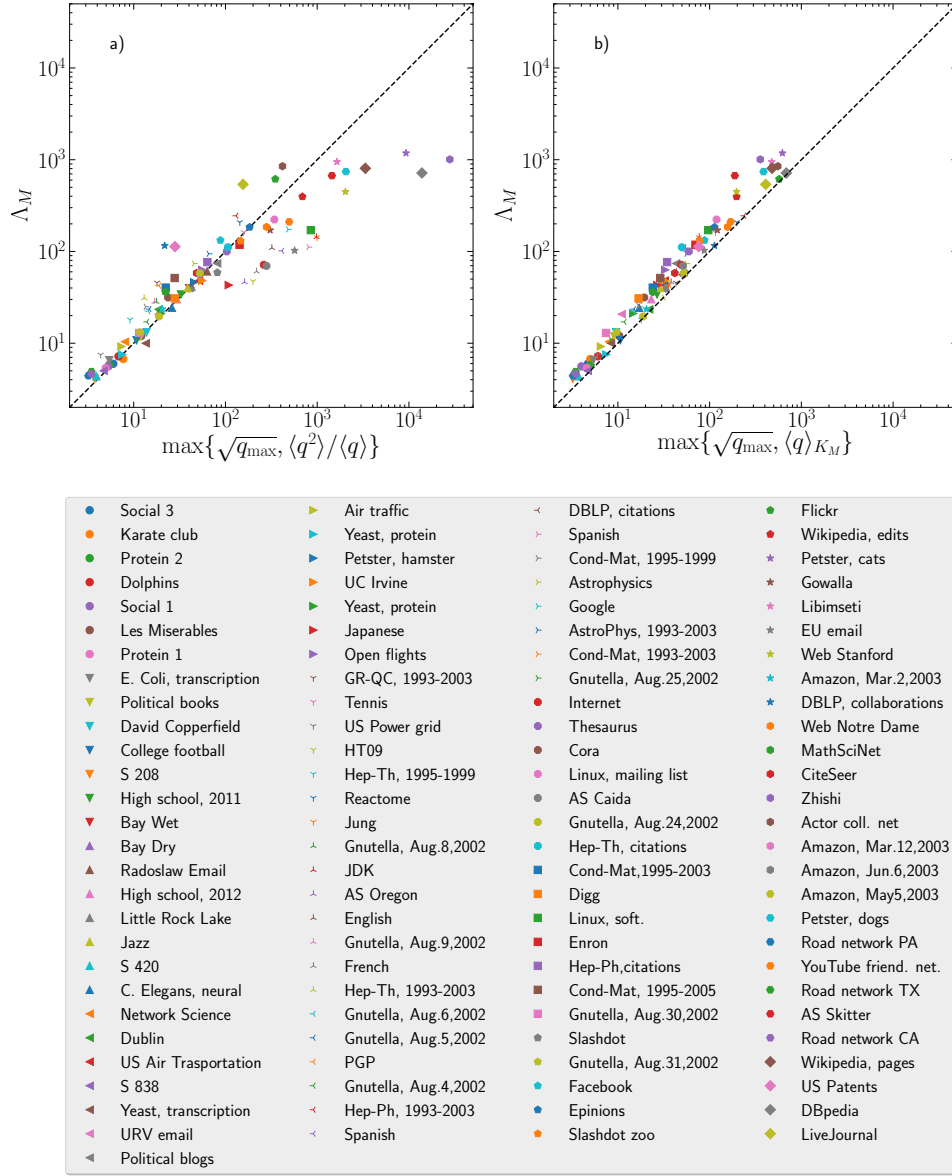


FIG. 2. (a) Largest eigenvalue  $\Lambda_M$  as a function of  $\max\{\sqrt{q_{\max}}, \langle q^2 \rangle / \langle q \rangle\}$  computed for 109 different real-world networks. (b) Largest eigenvalue  $\Lambda_M$  as a function of  $\max\{\sqrt{q_{\max}}, \langle q \rangle_{K_M}\}$  computed for the same real-world networks. Networks are ordered by increasing network size.

with largest degree in the network (the hub) and the scaling of  $\Lambda_M$  is given by  $\sqrt{q_{\max}}$ ; for  $\gamma < 5/2$ , on the other hand, the PEV becomes localized (in the sense discussed in Ref. [27]) on the core of nodes of maximum index  $K_M$  in the  $K$ -core decomposition of the network [28, 29] (see Appendix C); the associated LEV is then given by  $\langle q^2 \rangle / \langle q \rangle$ . This picture is confirmed in Fig. 1b, where we study the localization of the PEV, of components  $\{f_i\}$  assumed to be normalized as  $\sum_i f_i^2 = 1$ , in random uncorrelated networks. The analysis is performed by plotting the inverse participation ratio [27, 30, 31]  $Y_4(N)$  as a function of the network size (see Appendix B). As we can check, for  $\gamma > 5/2$ ,  $Y_4(N)$  goes to a constant for  $N \rightarrow \infty$ , indicating localization in a finite set of nodes, that coincide with the hub and its immediate neighbors. On the other hand, for  $\gamma < 5/2$  the inverse participation ratio decreases algebraically with network size, with an exponent  $\alpha$  smaller than 1, indicating localization in a sub-extensive set of nodes, which coincide with the maximum  $K$ -core [27]. Additional evidence is presented in Appendix D.

This observation can be interpreted in the following terms: The actual value of the LEV in the whole network is the result of the competition among two different subgraphs. The node with largest degree  $q_{\max}$  (the hub), together with its immediate neighbors, form a star graph which, in isolation, has a largest eigenvalue given by  $\Lambda_M^{(h)} = \sqrt{q_{\max}}$ . On the other hand, the maximum  $K$ -core, of index  $K_M$ , is a densely interconnected, essentially degree-homogeneous subgraph [26]. As such, its largest eigenvalue is given by its internal average degree,  $\Lambda_M^{(K_M)} \approx \langle q \rangle_{K_M}$ . In the case of uncorrelated networks, this average degree is well approximated

by  $\langle q^2 \rangle / \langle q \rangle$  [29]. These two subgraphs, and their respective largest eigenvalues,  $\Lambda_M^{(h)}$  and  $\Lambda_M^{(K_M)}$ , compete in order to set the scaling of the LEV of the whole network: The global LEV coincides with the subgraph LEV that is larger.

We hypothesize that for generic networks, and also for correlated ones, the same competition sets the overall LEV value. The largest eigenvalue of the star graph centered around the hub is trivially still equal to  $\sqrt{q_{\max}}$ . What changes in general topologies, and in particular in correlated networks, is the expression of the largest eigenvalue associated to the maximum  $K$ -core. One can realistically assume that the maximum  $K$ -core is in general degree-homogeneous (see the heterogeneity parameter of the maximum  $K$ -core or real-world networks in Table I, which is, except in one case, smaller than 1). What cannot be taken for granted in general is the identification between  $\langle q \rangle_{K_M}$  and  $\langle q^2 \rangle / \langle q \rangle$ . We thus conjecture that the LEV in generic networks can be expressed as

$$\Lambda_M \approx \max\{\sqrt{q_{\max}}, \langle q \rangle_{K_M}\}. \quad (4)$$

Eq. (4) is the central result of our paper. Note Eq. (4) is valid in full generality for any network if the approximation sign  $\approx$  is replaced by  $\geq$ , as Rayleigh's inequality guarantees that the largest eigenvalue of any subgraph is a lower bound for the whole network [1]. Our conjecture here is that this lower bound is also a very good approximation, in the sense that  $\Lambda_M$  differs from the lower bound by a factor of the order of few units.

Note that Eq. (4) includes Eq. (2) as a particular case when  $\langle q \rangle_{K_M} \approx \langle q^2 \rangle / \langle q \rangle$ , which is true in uncorrelated networks [29]. Moreover, Eq. (4) is in agreement with some known exact results for specific classes of networks. A simple example is provided by random  $q$ -regular-graphs. They have LEV equal to  $q$ , which is also the average degree of the max  $K$ -core, and is larger than  $\sqrt{q_{\max}} = \sqrt{q}$ . A less trivial example is given by random trees grown according to the linear preferential attachment rule (see Section IV). Bhamidi et al. [32] show that in this case the LEV is exactly  $\sqrt{q_{\max}}$ , the value predicted by Eq. (4) since by construction  $\langle q \rangle_{K_M} = 2$ . Another related exact result concerns the  $G(N, p)$  (Erdős-Rényi) random network, for which Krivelevich and Sudakov [33] have proven that  $\Lambda_M = (1 + o(1)) \max\{\sqrt{q_{\max}}, Np\}$  where the term  $o(1)$  tends to zero as the  $\max\{\sqrt{q_{\max}}, Np\}$  tends to infinity and  $Np$  is the average degree  $\langle q \rangle$ . According to Ref. [29], for Erdős-Rényi networks, the highest  $K$ -core is linear with the average degree,  $K_M \sim 0.78 \langle q \rangle$ , and the mean degree of the  $K$ -core depends weakly on the core and  $\langle q \rangle_K \simeq \langle q \rangle$ . Hence our Eq. (4) agrees with the result of Krivelevich and Sudakov for Erdős-Rényi networks.

In Fig. 2b we check the validity of the proposed generalized scaling for the LEV in the case of the 109 real-world networks considered above. Comparing with Fig. 2a, the generalized formula provides a much better overall fitting to the real value of the LEV than the original CLV expression, and therefore represents a better prediction for the behavior of this quantity. The overall improvement of our prediction versus the original CLV one can be established by comparing the absolute relative errors, with respect to actual measured LEVs, of the values predicted by Eq. (2) and Eq. (4), respectively. The average relative error for Eq. (2) is 1.213, with standard deviation 3.285, and a maximum of 26.686; for Eq. (4), the average is 0.282, with standard deviation 0.154 and maximum 0.719. We conclude that Eq. (4) provides an excellent approximation for the LEV value of an extremely broad variety of networks. Additional evidence of its predictive power is presented in the next Section.

Despite this vast generality, there are however particular classes of networks for which the lower bound is not tight and Eq. (4) is not a good approximation. These cases are examined in our discussion, Section VI.

#### IV. THE CASE OF LINEAR PREFERENTIAL ATTACHMENT NETWORKS

Growing network models provide a particularly interesting testbed for the conjecture presented above. We focus in particular on linear preferential attachment (LPA) networks [16, 34], generated starting from a fully connected nucleus of  $m + 1$  nodes and adding at every time step a new node with  $m$  new edges connected to  $m$  old nodes. For the vertex introduced at time  $t$ , each of its emanating edges is connected to an existing vertex  $s$ , introduced at time  $s < t$ , with probability

$$\Pi_s(t) = \frac{q_s(t) + a}{\sum_j [q_j(t) + a]}, \quad (5)$$

where  $q_s(t)$  is the degree, measured at time  $t$ , of the node introduced at time  $s$ . The factor  $a$  takes into account the possible initial attractiveness of each node, prior to receiving any connection. Large LPA networks are characterized by a power-law degree distribution  $P(k) \sim k^{-\gamma}$ , with a degree exponent  $\gamma = 3 + \frac{a}{m}$  [35] and average degree  $\langle q \rangle = 2m$ . It is thus possible to tune the degree exponent in the range  $2 < \gamma < \infty$  by changing the attractiveness parameter in the range  $-m < a < \infty$ . The power-law form extends up to the maximum degree  $q_{\max}$  that depends on  $N$  as  $q_{\max} \sim N^{1/(\gamma-1)}$  for all values of  $\gamma$ . LPA networks are further characterized by the presence of degree correlations [36]: The average degree of the nearest neighbors of nodes of degree  $q$ ,  $\bar{q}_{nn}(q)$  [37] is of the form  $\bar{q}_{nn}(q) \sim q^{-3+\gamma}$  for  $\gamma < 3$ , and  $\bar{q}_{nn}(q) \sim \ln q$  for  $\gamma > 3$  [35]. See Appendix E for a practical implementation of this model.

By their very construction LPA networks lack a nontrivial  $K$ -core structure, since the iterative procedure to determine  $K$ -shells for  $K > m$  removes all nodes by exactly reversing the growth process. Therefore, in LPA networks, all nodes belong to the same  $K = m$  shell, where  $m$  is the minimum degree in the network. We thus have  $\langle q \rangle_{K_M} = \langle q \rangle = 2m \ll \sqrt{q_{\max}}$  even for modest

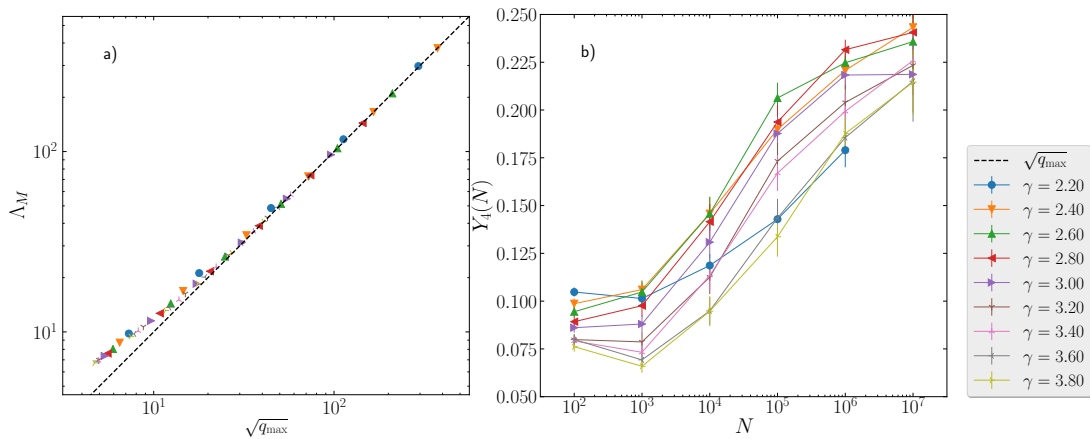


FIG. 3. **(a)** Largest eigenvalue  $\Lambda_M$  as a function of  $\sqrt{q_{\max}}$  in LPA networks with different degree exponent  $\gamma$ . **(b)** Inverse participation ratio  $Y_4(N)$  as a function of  $N$  in LPA networks with different degree exponent  $\gamma$ . Each point in both graphs corresponds to an average over 100 independent network realization. Error bars are smaller than symbol sizes.

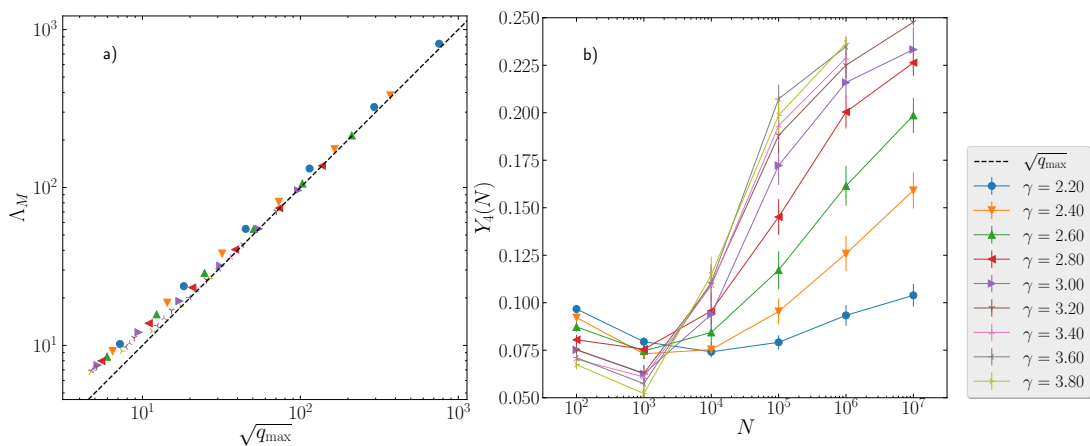


FIG. 4. **(a)** Largest eigenvalue  $\Lambda_M$  as a function of  $\sqrt{q_{\max}}$  in rewired LPA networks with different degree exponent  $\gamma$ . **(b)** Inverse participation ratio  $Y_4(N)$  as a function of  $N$  in rewired LPA networks with different degree exponent  $\gamma$ . Each point in both graphs corresponds to an average over 100 independent network realization. Error bars are smaller than symbol sizes.

values of  $N$ , and according to our generalized prediction, the LEV should be approximately  $\sqrt{q_{\max}}$  for all values of  $\gamma$ , in stark opposition to the original CLV formula, that still predicts in Eq. (3) different expressions for  $\gamma < 5/2$  and  $\gamma > 5/2$ . This scaling  $\Lambda_M \sim \sqrt{q_{\max}}$  has been exactly demonstrated for the case  $\gamma = 3$ , corresponding to the so-called Barabasi-Albert model [16] in Ref. [38]. Here we extend this form for all values of  $\gamma$  in LPA networks.

In Fig. 3a we plot the largest eigenvalue obtained in LPA networks with different size and degree exponent  $\gamma$ , as a function of  $\sqrt{q_{\max}}$ . As we can observe, after a short preasymptotic regime for small network sizes (small  $q_{\max}$ ),  $\Lambda_M$  grows as  $\sqrt{q_{\max}}$  for all values of  $\gamma$ , independently of the factor  $\langle q^2 \rangle / \langle q \rangle$ . Interestingly, for all values of  $\gamma$ , the LEV falls onto the same universal curve asymptotically approaching  $\sqrt{q_{\max}}$ , which indicates that this functional form is moreover independent of degree correlations, which change continuously with  $\gamma$  in LPA networks [35]. We conclude that, in perfect agreement with our conjecture, the spectral properties of LPA networks are ruled only by the hub. This implies additionally that the PEV is localized around the hub. This fact is verified in Fig. 3b, where we plot the inverse participation ratio  $Y_4(N)$  as a function of  $N$ . In Fig. 3b it turns out clearly that  $Y_4(N)$  goes to a constant for  $N \rightarrow \infty$ , for any degree exponent  $\gamma$  and for sufficiently large  $N$ , indicating that PEV always becomes localized on a set of nodes of finite size (not increasing with  $N$ ): The hub and its immediate neighbors. Further evidence about the localization is provided in Appendix F.

In LPA networks, the lack of a  $K$ -core structure is a fragile property, since reshuffling connections while preserving the degree of each node [39] may induce some  $K$ -core structure. This emerging  $K$ -core structure is however not able to restore the scaling predicted by Eq. (2) (see Appendix G). As Fig. 4a shows, reshuffling does not alter the overall behavior, apart from minimal changes: the LEV still scales asymptotically as  $\sqrt{q_{\max}}$  for any  $\gamma$ , while the PEV is still asymptotically localized around the hub, as the inverse participation ratio tending to a constant for large network sizes shows, Fig. 4b.

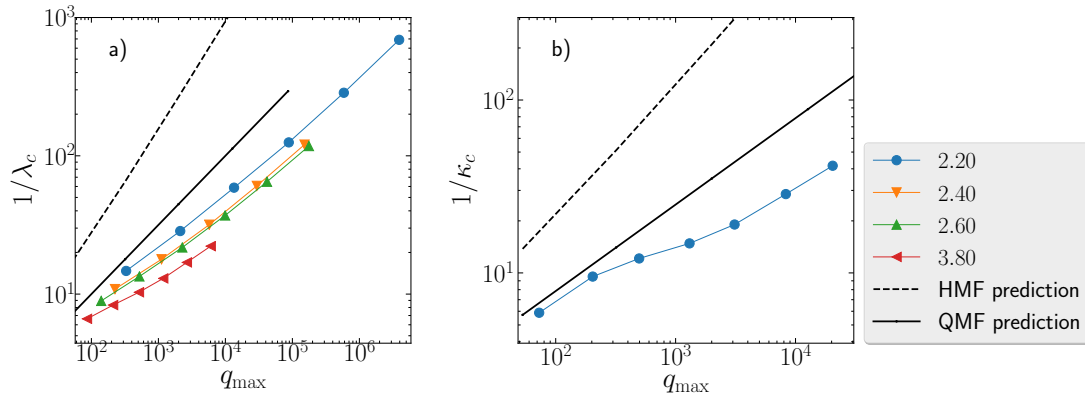


FIG. 5. (a) Numerical estimate of the inverse epidemic threshold  $1/\lambda_c$  in LPA as a function of  $q_{\max}$ , for various values of the exponent  $\gamma$ . We consider networks of sizes from  $N = 10^2$  to  $N = 10^8$ . (b) Numerical estimate of the synchronization threshold  $\kappa_c$  for  $\gamma = 2.2$  as a function of  $q_{\max}$ . System size ranges from  $N = 300$  to  $N = 300000$ . In both plots the dependence for  $\gamma = 2.2$  predicted by the QMF theory is represented by a thick dashed straight line, and the HMF prediction is represented by a dash-dotted line

## V. CONSEQUENCES FOR DYNAMICS ON NETWORKS

The spectral properties of the adjacency matrix determine the behavior of many dynamical processes mediated by topologically complex contact patterns [8–10, 22, 40]. Here we show the consequences that the topological properties uncovered above have for two highly relevant types of dynamics.

### A. Epidemic spreading

The Susceptible-Infected-Susceptible (SIS) model is one of the simplest and most fundamental models for epidemic spreading [41] (see Appendix H for details), showing an epidemic threshold  $\lambda_c$  separating a regime where epidemics get rapidly extinct from a regime where they affect a finite fraction of the system. The dependence of this threshold on the network topology is well approximated by the so-called Quenched Mean-Field theory (QMF) (see Appendix H), predicting it to be equal to the inverse of the LEV

$$\lambda_c = \frac{1}{\Lambda_M}. \quad (6)$$

Inserting into this expression the LEV scaling form given by Eq. (2) in the case of random uncorrelated static networks, we see that the threshold always vanishes on power-law distributed networks in the thermodynamic limit, with different scalings depending on the value of  $\gamma$  [22]. For  $\gamma < 5/2$  the expression coincides with the one predicted by the Heterogeneous Mean-Field (HMF) theory [42] (see Appendix H), while HMF theory is violated for  $\gamma > 5/2$ . In LPA networks  $\Lambda_M$  is, for any  $\gamma$ , given by  $\sqrt{q_{\max}}$ , so that Eq. (6) predicts a vanishing of the epidemic threshold qualitatively different from the one on uncorrelated networks for  $\gamma < 5/2$ . In particular, the approach to zero in the thermodynamic limit should be *slower* in LPA networks than in static uncorrelated networks with the same  $\gamma$ .

In order to check this picture, we perform numerical simulations of the SIS model on LPA networks of different degree exponent  $\gamma$ , and determine the threshold using the lifespan method (see Appendix H). In Fig. 5a we plot the numerically estimated threshold as a function of  $q_{\max}$ . We find that the theoretical expectation is followed only approximately: the slopes are smaller than 1 in all cases, the more so for larger values of  $\gamma$ . However, this discrepancy is a finite size effect: as the system size grows the effective slope grows. Asymptotically for large  $N$  the threshold always vanishes as  $\sqrt{q_{\max}}$ , at variance with what happens for uncorrelated static networks for  $\gamma < 5/2$ . The comparison with the slope predicted by HMF theory for  $\gamma = 2.2$  (dashed line) clearly shows the failure of the latter. Hence the remarkable conclusion that on LPA networks the epidemic threshold vanishes asymptotically for any  $\gamma$ , but it never vanishes as predicted by HMF theory, at odds with what happens on static uncorrelated networks.

In the case of real-world networks, our proposed estimate for the scaling of the largest eigenvalue again provides a much better overall prediction for the threshold in the SIS model, see Fig. 6, where we compare it with the original CLV prediction. As we can see, in cases where the CLV prediction is off by orders of magnitude, our improved scaling form leads to a much better threshold prediction. As an estimate of the overall goodness of the prediction, the mean relative error for the CLV predictions is 4.20 (standard deviation 11.92, maximum 52.02), while the predictions of Eq. (4) give much smaller values (mean 0.37, standard deviation 0.24, maximum 1.33).

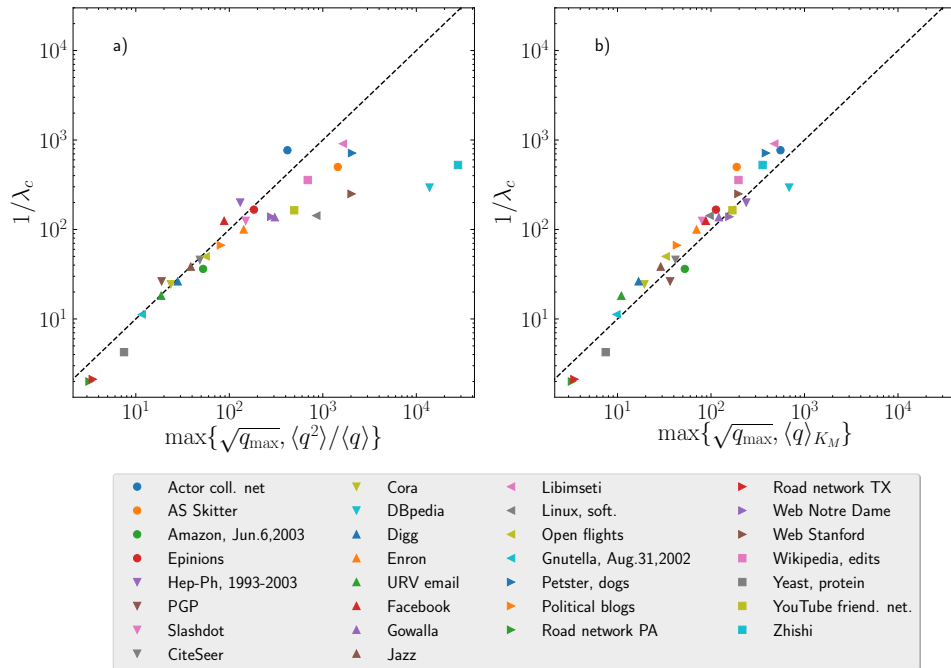


FIG. 6. (a) Numerical estimate of the inverse epidemic threshold  $1/\lambda_c$ , in a subset of the real-world networks considered, as a function of the inverse largest eigenvalue approximation  $\max\{\sqrt{q_{\max}}, \langle q^2 \rangle / \langle q \rangle\}$ . (b) Numerical estimate of the inverse epidemic threshold  $1/\lambda_c$  in real-world networks as a function of the inverse improved largest eigenvalue approximation  $\max\{\sqrt{q_{\max}}, \langle q \rangle_{K_M}\}$ . Data for the networks Zhishi, Web Notre Dame, Road network TX and Road network PA are lower bounds to the real threshold, due to computing time limitations.

## B. Synchronization

Kuramoto dynamics [43] (see Appendix I) is the paradigmatic model for the study of synchronization among weakly coupled oscillators, with applications ranging from neural networks to charge-density waves. Its behavior in networks has been investigated in great detail [44, 45], showing the existence of a synchronization threshold for a coupling parameter,  $\kappa_c$ , separating a random from a synchronized phase. Concerning the synchronization threshold, the standard approach is the one in Ref. [8], predicting a synchronized state to appear when the coupling  $\kappa$  among oscillators is larger than the critical value

$$\kappa_c = \frac{k_0}{\Lambda_M}, \quad (7)$$

where  $k_0 = 2/[\pi g(0)]$  and  $g(\omega)$  is the frequency distribution of individual oscillators (see Appendix I). To assess whether the generalized scaling just uncovered for  $\Lambda_M$  on LPA networks has effects also for these dynamics, we perform simulations of the Kuramoto model on growing networks and determine the critical coupling  $\kappa_c$  (see Appendix I for details).

Fig. 5b clearly shows that also for these dynamics the prediction given by the inverse of the LEV is qualitatively correct and, as a consequence, for  $\gamma < 5/2$  the threshold vanishes more slowly than what is predicted for random uncorrelated networks. We conclude that also in this case the nature of the growing network, and in particular the lack of a  $K$ -core structure, has profound consequences for the dynamics mediated by the contact network.

## VI. DISCUSSION

The generalized CLV conjecture we have exposed allows to fully clarify the physical origin of the properties of the adjacency matrix largest eigenpair in complex networks. There are two subgraphs which determine the LEV and the PEV in a large complex network: the hub with its spokes and the densely mutually interconnected set of nodes singled out as the maximum  $K$ -core [46]. Each of these two subgraphs has (in isolation) an associated LEV: the hub is the center of a star graph and therefore  $\Lambda_M^{(h)} = \sqrt{q_{\max}}$ ; the maximum  $K$ -core is a homogeneous graph and therefore  $\Lambda_M^{(K_M)} \simeq \langle q \rangle_{K_M}$ . The LEV of the global topology is simply given by the largest of the two. In uncorrelated static networks the growth with  $N$  of the two individual LEVs depends on  $\gamma$  and this gives rise to the change of behavior occurring for  $\gamma = 5/2$ , Eq. (3). In growing LPA networks the  $K$ -core structure



is by construction absent: The spectral properties are dictated only by the hub (and this remains true also after reshuffling). In networks of any origin (and any correlation level), the relation between the average degree of the max  $K$ -core and  $\langle q^2 \rangle / \langle q \rangle$  may break down. However it is still true that the LEV value is the largest between  $\Lambda_M^{(h)}$  and  $\Lambda_M^{(K_M)}$ .

This conjecture is clearly not a proof. However, the understanding of its conceptual origin allows to predict that it should hold for practically all real-world networks. Various different mechanisms may lead to its breakdown. There could be an *inhomogeneous* max  $K$ -core in the network, so that  $\Lambda_M^{(K_M)}$  is very different from  $\langle q \rangle_{K_M}$ . There could be a third, different, type of subgraph, characterized by a LEV larger than both the others. Or the whole graph could have a LEV larger than the LEV of any proper subgraph. An example of this last case is the complete bipartite network  $K_{p,q}$ : its LEV is  $\sqrt{pq}$  [1], which can be much larger (assuming  $p \leq q$ ) than the value  $\max\{\sqrt{q}, p\}$  predicted by Eq. (4). All these mechanisms are in principle possible; however they appear to be unlikely in real self-organized networks.

Our findings about spectral properties have immediate implications in several contexts. We have shown that properties of dynamical processes as general as epidemics and synchronization are deeply affected by which subgraph determines the LEV. For example, another effect that can be immediately predicted, is that removing the hub may completely disrupt the dynamics when the LEV is given by  $\Lambda_M^{(h)}$  while being practically inconsequential in the other case. Similar consequences are expected to occur in general [9–11, 40]. Another context where these results may have implications is for centrality measures, many of which are variations of the eigenvalue centrality [6, 47]. Finally, it is worth to remark that the example of linear preferential attachment networks clearly points out that the way a network is built may have deep and unexpected implications for its structure and its functionality.

### ACKNOWLEDGMENTS

We acknowledge financial support from the Spanish MINECO, under projects FIS2013-47282-C2- 2 and FIS2016-76830-C2-1-P. R.P.-S. acknowledges additional financial support from ICREA Academia, funded by the Generalitat de Catalunya.

### Appendix A: Applicability of CLV exact results to finite networks

The exact result proved by Chung, Lu and Vu in Ref. [17], namely Eq. (1), can be rewritten as

$$\Lambda_M = \begin{cases} a_1 \sqrt{q_{\max}} & \text{if } \frac{\langle q^2 \rangle}{\langle q \rangle \sqrt{q_{\max}}} < \frac{1}{\ln^2(N)} \\ a_2 \frac{\langle q^2 \rangle}{\langle q \rangle} & \text{if } \frac{\langle q^2 \rangle}{\langle q \rangle \sqrt{q_{\max}}} > \ln(N) \end{cases}. \quad (\text{A1})$$

It therefore provides a prediction for the value of the LEV if the ratio

$$\zeta(\gamma, N) \equiv \frac{\langle q^2 \rangle}{\langle q \rangle \sqrt{q_{\max}}} \quad (\text{A2})$$

is larger than  $\ln(N)$  or smaller than  $1/\ln^2(N)$ . For very large systems both  $\langle q^2 \rangle / \langle q \rangle$  and  $\sqrt{q_{\max}}$  diverge and, if they scale with  $N$  with different exponents (i.e.  $\gamma \neq 5/2$ ), the logarithmic factors are not asymptotically relevant: either the first or the second of the conditions in Eq. (1) is fulfilled. However, for finite values of  $N$  there is a sizeable interval such that Eq. (1) does not strictly apply. In the case of uncorrelated power-law networks with distribution  $P(q) = (\gamma - 1)m^{\gamma-1}q^{-\gamma}$ , we have, in the continuous degree approximation

$$\zeta(\gamma, N) = \frac{\gamma - 2}{3 - \gamma} \frac{m}{\sqrt{q_{\max}}} \left[ \left( \frac{q_{\max}}{m} \right)^{3-\gamma} - 1 \right], \quad (\text{A3})$$

where  $q_{\max} = N^{1/2}$  for  $\gamma < 3$  and  $q_{\max} = N^{1/(\gamma-1)}$  for  $\gamma > 3$ ,  $m$  is the minimum degree, which we take  $m = 3$ , and in the evaluation of  $\langle q^2 \rangle$  we have taken the maximum degree  $q_{\max}$  into account. Evaluating numerically  $\zeta(\gamma, N)$  we can compute for every value of  $\gamma$  the minimum value of  $N$  for the exact expression Eq. (1) to apply. For  $\gamma < 5/2$ ,  $\zeta(\gamma, N)$  diverges with  $N$ : the prediction  $\Lambda_M \approx \langle q^2 \rangle / \langle q \rangle$  in Eq. (1) applies for  $N > N_{\min}$  defined by  $\zeta(\gamma, N_{\min}) = \ln(N_{\min})$ . On the other hand, for  $\gamma > 5/2$ ,  $\zeta(\gamma, N)$  tends to zero as the system size diverges. Hence the prediction  $\Lambda_M \approx \sqrt{q_{\max}}$  in Eq. (1) applies for  $N > N_{\min}$ , defined in this case by  $\zeta(\gamma, N_{\min}) = 1/\ln^2(N_{\min})$ . In Fig. 7 we plot  $N_{\min}$  as a function of  $\gamma$ . From the figure it turns out that the exact theoretical prediction Eq. (1) holds only for extremely large size (at least  $N > 10^{11}$ , but the bound is much larger for almost all values of  $\gamma$ ). Networks of such size cannot be simulated with current computer resources. An improved analysis in Ref. [17] replaces  $\ln(N)$  by  $\ln(N)^{1/2}$  and  $\ln(N)^2$  by  $\ln(N)^{3/2}$  in Eq. (1). A similar analysis as performed above indicates that

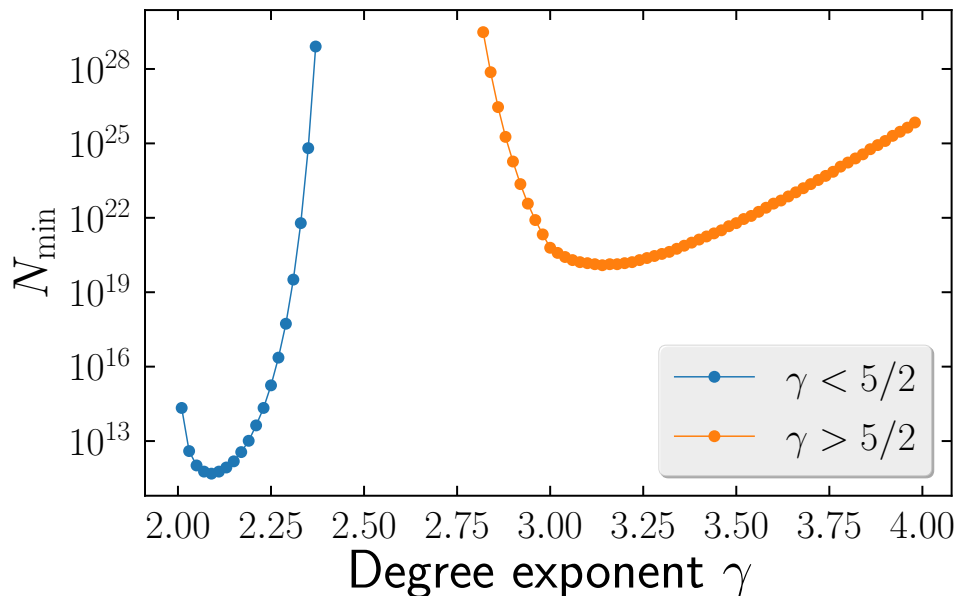


FIG. 7. Minimum sizes  $N_{\min}$  for the validity of Eq. (1) in uncorrelated power-law networks as a function of the degree exponent  $\gamma$ . Values in the vicinity of  $\gamma = 5/2$  not plotted are all larger than  $10^{30}$ .

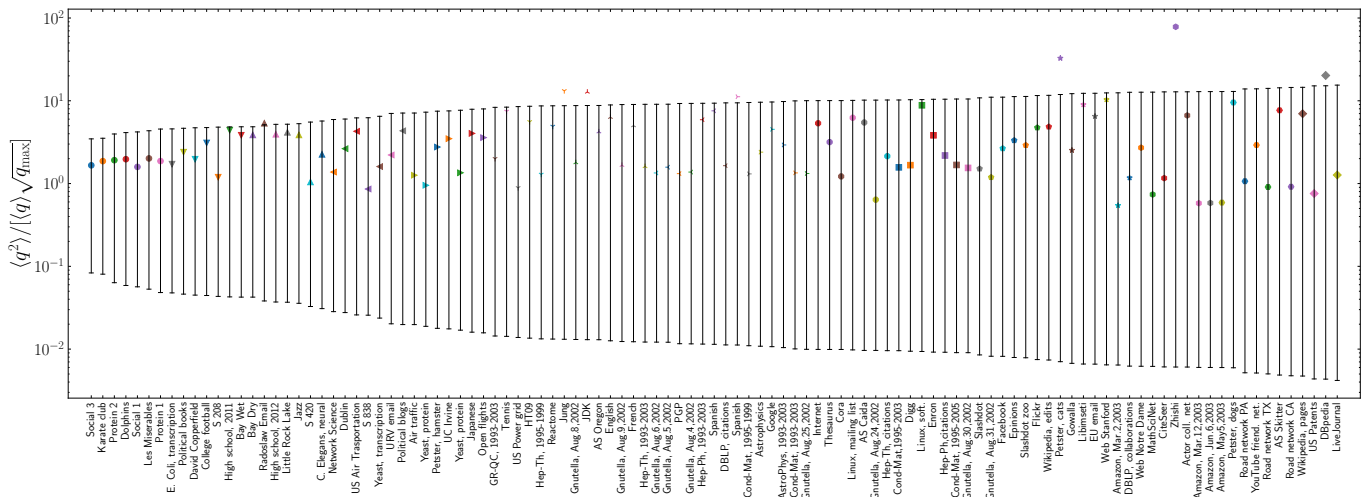


FIG. 8. For each of the real-world networks considered, we plot in log scale a line indicating the interval where Eq. (1) does not make any prediction. The symbols indicate the actual value of  $\langle q^2 \rangle / (\langle q \rangle \sqrt{q_{\max}})$  for each network.

this corrected version holds for sizes at least  $N > 3 \times 10^7$ , which is very close to the limit allowed by present computation systems.

In the case of the real-world networks considered, we plot in Fig. 8 along the  $y$ -axis a line between  $\ln(N)$  and  $1/\ln^2(N)$ , indicating the interval of values of  $\langle q^2 \rangle / (\langle q \rangle \sqrt{q_{\max}})$  where Eq. (1) does not strictly apply. The symbols indicate the actual value of the ratio  $\langle q^2 \rangle / (\langle q \rangle \sqrt{q_{\max}})$  in each network. It turns out that for 102 networks out of 109 the actual value falls in the inapplicability interval. Hence for the vast majority of real networks the exact result in Eq. (1) does not, strictly speaking, allow to make any prediction.

## Appendix B: Eigenvector localization and the inverse participation ratio

The concept of the localization of the principal eigenvector  $\{f_i\}$  translates in determining whether the value of its normalized components (satisfying  $\sum_i f_i^2 = 1$ ) is evenly distributed among all nodes in the network or it attains a large value on some subset

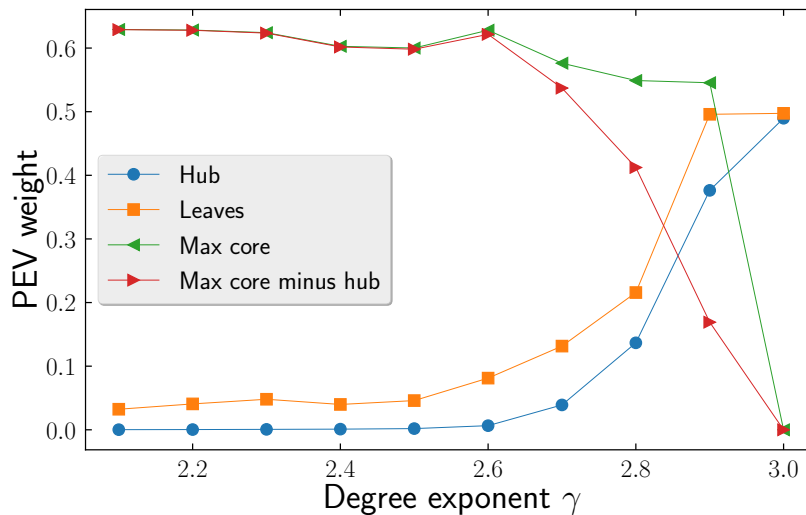


FIG. 9. PEV weight concentrated on various subgraphs for UCM networks of size  $N = 10^7$  with different values of  $\gamma$ .

of nodes  $V$  and is much smaller in all the rest. In the first case  $f_i \sim N^{-1/2}, \forall i$  and the network is not localized. In the second case  $f_i \sim N_V^{-1/2}$ , for  $i \in V$  and  $f_i \sim 0$ , for  $i \notin V$ , where  $N_V$  is the size of the localization subset  $V$ .

The presence of localization in the PEV can be easily assessed in ensembles of networks of variable size  $N$  by studying the inverse participation ratio (IPR), defined as [30, 31]

$$Y_4(N) = \sum_{i=1}^N [f_i]^4, \quad (\text{B1})$$

as a function of  $N$ , and fitting its behavior to a power-law decay of the form [27]

$$Y_4(N) \sim N^{-\alpha}. \quad (\text{B2})$$

If the PEV is delocalized, with  $f_i \sim N^{-1/2}, \forall i$ , the exponent  $\alpha$  is equal to 1. Any exponent  $\alpha < 1$  indicates the presence of some form of eigenvector localization, taking place in a sub-extensive set of nodes, of size  $N_V \sim N^\alpha$ . In the extreme case of localization on a single node, or a set of nodes with fixed size, we have  $\alpha = 0$  and  $Y_4(N) \sim \text{const.}$

### Appendix C: The $K$ -core decomposition

The  $K$ -core decomposition [28] is an iterative procedure to classify vertices of a network in layers of increasing density of mutual connections. Starting with the whole graph one removes the vertices with only one connection (degree  $q = 1$ ). This procedure is then repeated until only nodes with degree  $q \geq 2$  are left. The removed nodes constitute the  $K=1$ -shell and those remaining are the  $K=2$ -core. At the next step all vertices with degree  $q = 2$  are removed, thus leaving the  $K=3$ -core. The procedure is repeated iteratively. The maximum  $K$ -core (of index  $K_M$ ) is the set of vertices such that one more iteration of the procedure removes all of them. Notice that all vertices of the  $K$ -core of index  $K$  have degree larger than or equal to  $K$ .

### Appendix D: Different localizations for UCM networks

For UCM networks the localization of the PEV in different subgraphs depending on whether  $\gamma$  is larger or smaller than  $5/2$  can be exposed by plotting the weights concentrated on the subgraphs as a function of  $\gamma$  (see Fig. 9). In this figure we have set the weight of the maximum  $K$ -core equal to zero for  $\gamma = 3$ , since by construction it coincides with the whole network, and trivially contains all the weight for the PEV.

It is clear that for  $\gamma < 5/2$  the weight is concentrated on the max  $K$ -core, while the hub plays no role. For  $\gamma > 5/2$  the opposite scenario applies: the hub plus its nearest neighbors (leaves) bear most of the PEV weight, while the max  $K$ -core (or the max  $K$ -core minus the hub, in case the latter belongs to the former) has vanishing weight concentrated on it. Strong finite size effects smoothen the change of behavior for  $\gamma$  between  $5/2$  and  $3$ ; but changing the system size (not shown) one can extrapolate that for asymptotically large systems the picture is the one just described.

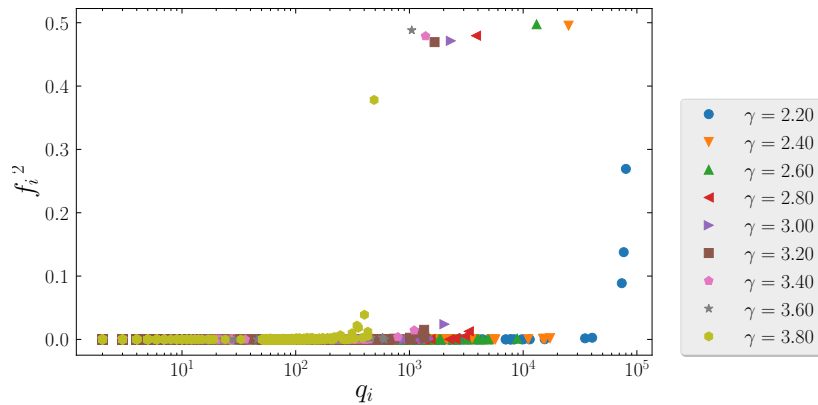


FIG. 10. Scatter plot of  $f_i^2$  as a function of the degree  $q_i$  in LPA networks of different degree exponent  $\gamma$ . Network size  $N = 10^6$ .

### Appendix E: Building linear preferential attachment networks

Given the mapping of LPA networks with the Price model [48], LPA networks can be easily constructed with the following simplified algorithm [5]: Every time step a new node is added, with  $m$  new edges. Each one of them is connected to an old node, chosen uniformly at random, with probability  $\phi = a/(a+m)$ ; otherwise, with the complementary probability  $1-\phi = m/(a+m)$ , the edge is connected to a node chosen with probability proportional to its in-degree  $q_s(t) - m$ . In our simulations we consider LPA networks with minimum degree  $m = 2$  and varying  $\gamma$ , for network sizes ranging from  $N = 10^2$  up to  $N = 10^8$ . Topological and spectral properties of LPA networks are computed averaging over 100 different network configurations for each value of  $\gamma$  and  $N$ .

### Appendix F: Principal eigenvector localization in linear preferential attachment networks

A direct way to observe PEV localization consists in plotting the square of the components  $f_i^2$  as a function of the node degree  $q_i$ , Fig. 10. As we can see from this figure, for all values of  $\gamma$  the component of the PEV associated to the largest values of  $q$  have a macroscopic weight, indicating localization of the PEV in the hubs. This plot presents evidence of a further difference of LPA networks with respect to random uncorrelated networks. In this case, and for  $\gamma < 5/2$ , it is possible to show that the PEV components approach in static networks the form obtained within the annealed network approximation [49], which is given by [27].

$$f_i^{\text{an}} = \frac{q_i}{[N \langle q^2 \rangle]^{1/2}}. \quad (\text{F1})$$

As we can see in Fig. 10, this linear behavior is not present in the data from LPA networks, even for small  $\gamma$  values.

### Appendix G: $K$ -core structure in reshuffled linear preferential attachment networks

The lack of  $K$ -core structure of LPA networks arises from its peculiar growing nature, in which nodes with minimum degree  $m$  are sequentially attached to the network. This property is not robust, however, since a simple reshuffling procedure can destroy it, inducing a non-trivial  $K$ -core structure. In Fig. 11 we show the average maximum core index,  $\langle K_M \rangle$ , as a function of the network size, computed from LPA networks with different degree exponent, in which edges have been reshuffled according to the degree preserving edge rewiring process described in Ref. [39]. As we can observe, for  $\gamma \geq 3$ , the reshuffling process is not able to induce a substantial  $K$ -core structure. This occurs because the reshuffling destroys correlations but uncorrelated networks with  $\gamma > 3$  have essentially no  $K$ -core structure [29]. For  $\gamma < 3$ , on the other hand, the  $K$ -core structure generated by reshuffling is robust, with an average maximum core index increasing as a power-law with network size [29].

The maximum  $K$ -core resulting from the reshuffling of LPA networks has an average degree,  $\langle q \rangle_{K_M}$ , that depends on the maximum degree  $q_{\text{max}}$ , see Fig. 12. However, since the hub has degree much larger than  $N^{1/2}$ , the network does not become uncorrelated even upon randomization and  $\langle q \rangle_{K_M}$  is always smaller than  $\sqrt{q_{\text{max}}}$ . Hence the properties of the largest eigenpair are always dictated by the hub, as in the original LPA networks.

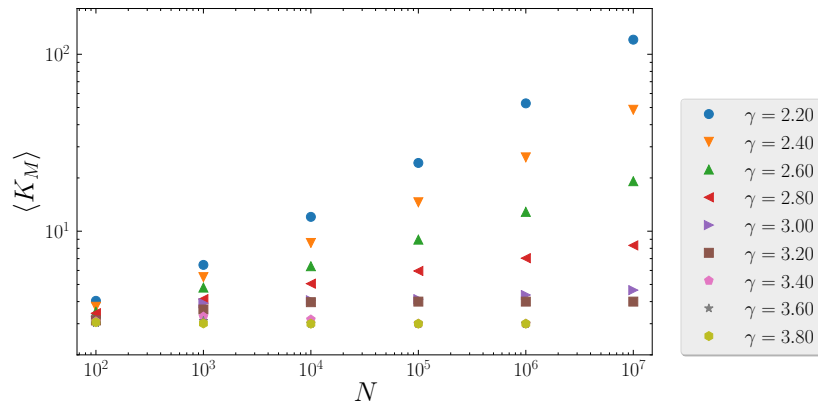


FIG. 11. Average maximum core index,  $\langle K_M \rangle$  as a function of network size for reshuffled LPA networks with different degree exponent  $\gamma$ . Error bars are smaller than symbol sizes.

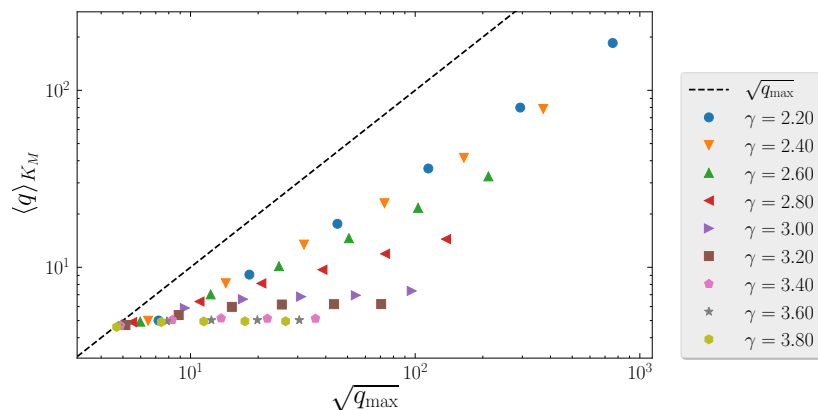


FIG. 12. Average maximum core index,  $\langle q \rangle K_M$  as a function of network size for reshuffled LPA networks with different degree exponent  $\gamma$ . Error bars are smaller than symbol sizes.

### Appendix H: Susceptible-Infected-Susceptible epidemic dynamics

The Susceptible-Infected-Susceptible (SIS) model is the simplest model designed to capture the properties of diseases that do not confer immunity [50]. In the SIS model, individuals can be in either of two states, susceptible or infected. Susceptible individuals become infected through a contact with an infected individual at rate  $\beta$ , while infected individuals heal spontaneously at rate  $\mu$ . As a function of the parameter  $\lambda = \beta/\mu$ , the model shows a non-equilibrium phase transition between an active, infected phase for  $\lambda > \lambda_c$ , and an inactive, healthy phase for  $\lambda \leq \lambda_c$ . Interest is placed on the location of the so-called epidemic threshold  $\lambda_c$ , and on its dependence on the topological properties of the network under consideration [51].

Early theoretical approaches to the SIS dynamics were based on the so-called Heterogeneous Mean-Field (HMF) theory [42, 52], which neglects both dynamical and topological correlations by replacing the actual structure of the network, as given by the adjacency matrix, by an annealed version in which edges are constantly rewired, while preserving the degree distribution  $P(q)$ . Within this annealed network approximation [53], a threshold for uncorrelated networks is obtained of the form  $\lambda_c = \langle q \rangle / \langle q^2 \rangle$ . An improvement over this approximate theory is given by Quenched Mean-Field (QMF) theory [7], which, while still neglecting dynamical correlations, takes into account the full structure of the adjacency matrix. Within this approximation, the threshold is given by the inverse of the largest eigenvalue of the adjacency matrix,  $\lambda_c = 1/\Lambda_M$ . Recent and intense activity, based on more sophisticated approaches [22, 54, 55] has shown that on uncorrelated static networks this result is essentially asymptotically correct.

In order to determine  $\lambda_c$  numerically, we resort to the lifespan method [55, 56], which is not affected by the drawbacks that make the consideration of susceptibility unwieldy [54]. Simulations start with only the hub infected. For each run one keeps track of the coverage, i.e. fraction of different nodes which have been touched at least once by the infection. In an infinite network this quantity is vanishing for  $\lambda \leq \lambda_c$ , while it tends asymptotically to 1 in the active region of the phase-diagram. In finite networks one can set a threshold  $c$  (we choose  $c = 0.5$ ) and consider all runs that reach a coverage larger than  $c$  as endemic. The average

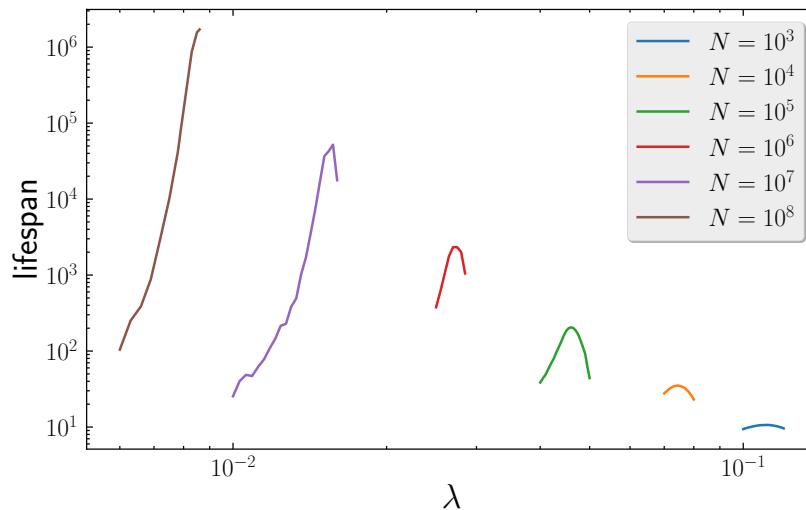


FIG. 13. Average lifespan vs spreading rate  $\lambda_c$  of SIS epidemics starting from a single infected node (the hub) and reaching the healthy absorbing state before the coverage reaches the threshold value  $c = 0.5$ . Data are for LPA networks with  $\gamma = 2.6$  and various system size  $N$ .

lifespan  $\langle T \rangle$  restricted only to nonendemic runs plays the role of a susceptibility: The position of the threshold is estimated as the value of  $\lambda$  for which  $\langle T \rangle$  reaches a peak, see Fig. 13.

#### Appendix I: Kuramoto synchronization dynamics

The Kuramoto model [43, 45] describes the dynamics of a collection of weakly coupled nearly identical oscillators. If they are placed on the nodes of a network with adjacency matrix  $A_{ij}$  the equation of motion reads

$$\dot{\theta}_i = \omega_i + \kappa \sum_j A_{ij} \sin(\theta_j - \theta_i), \quad (11)$$

where  $\kappa$  is a coupling constant and  $\omega_i$  is a quenched random variable (natural frequency), whose distribution  $g(\omega)$  is taken here uniform between  $-1$  and  $1$ . In the initial condition the phases  $\theta_i$  are uniformly random between  $0$  and  $2\pi$ . Defining the global order parameter as

$$r = \left| \frac{1}{N} \sum_i e^{-I\theta_i} \right|, \quad (12)$$

where  $I$  is the imaginary unit, one finds that there is a critical threshold  $\kappa_c$  separating a disordered phase where  $r = 0$  (in the thermodynamic limit) from a synchronized phase with  $r > 0$ . A QMF-like theory for the Kuramoto model [8] predicts a critical point  $\kappa_c = k_0/\Lambda_M$ , where  $k_0 = 2/[\pi g(0)] = 4/\pi$ , the last equality holding because of the uniform distribution of natural frequencies  $g(\omega)$ .

The value of the critical threshold is numerically determined in finite networks by computing the susceptibility,  $\chi_K(\kappa) = N(\langle r^2 \rangle - \langle r \rangle^2)$ , which shows a peak for  $\kappa = \kappa_c$ .

Appendix J: Supplementary Table

Network	$N$	$\langle q \rangle$	$q_{\max}$	$\chi$	$r$	$K_M$	$N_{K_M}$	$\langle q \rangle_{K_M}$	$\chi_{K_M}$
Social 3	32	5.0	13	0.2	-0.1194	4	17	4.7	0.0891
Karate club	34	4.6	17	0.7	-0.4756	4	9	5.0	0.0400
Protein 2	53	4.6	8	0.2	0.2088	4	29	5.0	0.0421
Dolphins	62	5.1	12	0.3	-0.0436	4	35	6.1	0.0681
Social 1	67	4.2	11	0.2	0.1031	4	5	4.0	0.0000
Les Miserables	77	6.6	36	0.8	-0.1652	9	12	10.3	0.0083
Protein 1	95	4.5	7	0.1	0.1293	3	83	4.6	0.0779
E. Coli, transcription	97	4.4	10	0.2	0.4116	4	20	5.4	0.0562
Political books	105	8.4	25	0.4	-0.1279	6	40	9.1	0.1152
David Copperfield	112	7.6	49	0.8	-0.1293	6	43	9.5	0.2661
College football	115	10.7	12	0.0	0.1624	8	113	10.6	0.0067
S 208	122	3.1	10	0.2	-0.0020	2	108	3.2	0.1911
High school, 2011	126	27.1	55	0.2	0.0829	21	33	26.7	0.0157
Bay Wet	128	32.4	110	0.2	-0.1117	23	80	33.2	0.0869
Bay Dry	128	32.9	110	0.2	-0.1044	24	73	32.7	0.0680
Radoslaw Email	167	38.9	139	0.7	-0.2952	36	80	51.4	0.0559
High school, 2012	180	24.7	56	0.2	0.0464	18	57	23.1	0.0246
Little Rock Lake	183	26.6	105	0.6	-0.2664	23	64	33.2	0.0819
Jazz	198	27.7	100	0.4	0.0202	29	30	29.0	0.0000
S 420	252	3.2	14	0.2	-0.0059	2	226	3.3	0.2115
C. Elegans, neural	297	14.5	134	0.8	-0.1632	10	118	17.1	0.2558
Network Science	379	4.8	34	0.7	-0.0817	8	9	8.0	0.0000
Dublin	410	13.5	50	0.4	0.2258	17	32	21.9	0.0182
US Air Transportation	500	11.9	145	3.5	-0.2679	29	34	32.5	0.0023
S 838	512	3.2	22	0.3	-0.0300	2	462	3.3	0.2373
Yeast, transcription	662	3.2	71	3.2	-0.4098	3	168	4.9	0.3653
URV email	1133	9.6	71	0.9	0.0782	11	12	11.0	0.0000
Political blogs	1222	27.4	351	2.0	-0.2213	36	55	43.2	0.0139
Air traffic	1226	3.9	34	0.9	-0.0152	4	106	6.5	0.1886
Yeast, protein	1458	2.7	56	1.7	-0.2095	5	6	5.0	0.0000
Petster, hamster	1788	14.0	272	2.3	-0.0889	20	130	31.4	0.1399
UC Irvine	1893	14.6	255	2.8	-0.1880	20	201	32.1	0.1512
Yeast, protein	2172	6.0	215	2.3	-0.0552	10	14	11.6	0.0093
Japanese	2698	5.9	725	17.3	-0.2590	15	52	22.5	0.1110
Open flights	2905	10.8	242	4.2	0.0489	28	38	32.8	0.0079
GR-QC, 1993-2003	4158	6.5	81	1.8	0.6392	43	44	43.0	0.0000
Tennis	4338	37.7	451	3.2	0.0033	79	308	115.7	0.0779
US Power grid	4941	2.7	19	0.5	0.0035	5	12	6.0	0.0139
HT09	5352	6.9	1287	28.0	-0.4308	10	319	18.0	1.0255
Hep-Th, 1995-1999	5835	4.7	50	0.9	0.1852	18	19	18.0	0.0000
Reactome	5973	48.8	855	1.9	0.2414	176	209	197.8	0.0036
Jung	6120	16.4	5655	59.3	-0.2327	65	135	76.2	0.0359
Gnutella, Aug.8,2002	6299	6.6	97	1.7	0.0355	10	268	17.0	0.6928
JDK	6434	16.7	5923	57.9	-0.2230	65	135	76.2	0.0359
AS Oregon	6474	3.9	1458	41.4	-0.1818	12	20	15.5	0.0370
English	7377	12.0	2568	25.8	-0.2366	37	112	54.7	0.0991
Gnutella, Aug.9,2002	8104	6.4	102	1.6	0.0331	10	315	17.1	0.8434
French	8308	5.7	1891	37.0	-0.2330	17	45	23.2	0.0490
Hep-Th, 1993-2003	8638	5.7	65	1.3	0.2389	31	32	31.0	0.0000
Gnutella, Aug.6,2002	8717	7.2	115	1.0	0.0516	9	175	14.6	0.3343
Gnutella, Aug.5,2002	8842	7.2	88	1.1	0.0146	9	238	15.0	0.5772
PGP	10680	4.6	205	3.1	0.2382	31	41	36.5	0.0057
Gnutella, Aug.4,2002	10876	7.4	103	0.9	-0.0132	7	365	11.8	0.3184
Hep-Ph, 1993-2003	11204	21.0	491	5.2	0.6295	238	239	238.0	0.0000
Spanish	11558	7.4	2986	60.4	-0.2819	30	74	42.7	0.0683
DBLP, citations	12495	7.9	709	4.5	-0.0461	12	916	21.5	0.5223
Spanish	12643	8.7	5169	91.8	-0.2897	30	88	44.9	0.1029
Cond-Mat, 1995-1999	13861	6.4	107	1.1	0.1571	17	18	17.0	0.0000
Astrophysics	14845	16.1	360	1.8	0.2277	56	57	56.0	0.0000

Google	15763	18.9	11401	46.8	-0.1215	102	206	106.3	0.0129
AstroPhys, 1993-2003	17903	22.0	504	2.0	0.2013	56	57	56.0	0.0000
Cond-Mat, 1993-2003	21363	8.5	279	1.6	0.1253	25	26	25.0	0.0000
Gnutella, Aug.25,2002	22663	4.8	66	1.2	-0.1734	5	6091	8.4	0.1481
Internet	22963	4.2	2390	61.0	-0.1984	25	70	38.2	0.0910
Thesaurus	23132	25.7	1062	3.0	-0.0477	34	3644	59.4	0.5376
Cora	23166	7.7	377	2.1	-0.0553	13	25	17.4	0.0329
Linux, mailing list	24567	12.9	2989	25.5	-0.1852	91	157	119.1	0.0287
AS Caida	26475	4.0	2628	68.5	-0.1946	22	64	33.4	0.0688
Gnutella, Aug.24,2002	26498	4.9	355	1.4	-0.0078	5	7479	8.8	0.3446
Hep-Th, citations	27400	25.7	2468	3.1	-0.0305	37	52	44.1	0.0068
Cond-Mat,1995-2003	27500	8.4	202	1.6	0.1663	24	25	24.0	0.0000
Digg	29652	5.7	283	3.9	0.0027	9	1339	16.8	0.4619
Linux, soft.	30817	13.8	9338	60.6	-0.1747	23	439	41.3	0.7557
Enron	33696	10.7	1383	12.3	-0.1165	43	275	70.1	0.1584
Hep-Ph,citations	34401	24.5	846	1.6	-0.0064	30	40	34.4	0.0054
Cond-Mat, 1995-2005	36423	9.4	277	2.0	0.1776	29	30	29.0	0.0000
Gnutella, Aug.30,2002	36646	4.8	55	1.4	-0.1038	7	14	7.0	0.0000
Slashdot	51083	4.6	2915	16.9	-0.0347	14	736	25.8	0.4878
Gnutella, Aug.31,2002	62561	4.7	95	1.5	-0.0927	6	1004	9.1	0.1253
Facebook	63392	25.8	1098	2.4	0.1768	52	701	88.1	0.1538
Epinions	75877	10.7	3044	16.2	-0.0406	67	485	113.0	0.1608
Slashdot zoo	79116	11.8	2534	11.4	-0.0746	54	129	77.8	0.0590
Flickr	105722	43.8	5425	7.0	0.2468	573	574	573.0	0.0000
Wikipedia, edits	113123	35.8	20153	18.3	-0.0651	145	936	196.7	0.1049
Petster, cats	148826	73.2	80634	125.9	-0.1642	419	1283	621.7	0.0766
Gowalla	196591	9.7	14730	30.7	-0.0293	51	185	76.0	0.0957
Libimseti	220970	156.0	33389	9.5	-0.1390	273	4110	475.6	0.2285
EU email	224832	3.0	7636	186.7	-0.1892	37	292	63.1	0.1730
Web Stanford	255265	15.2	38625	132.5	-0.1156	71	387	112.2	0.3004
Amazon, Mar.2,2003	262111	6.9	420	0.6	-0.0025	6	286	6.6	0.0389
DBLP, collaborations	317080	6.6	343	2.3	0.2665	113	114	113.0	0.0000
Web Notre Dame	325729	6.7	10721	40.9	-0.0534	155	1367	157.3	0.0591
MathSciNet	332689	4.9	496	2.3	0.1030	24	25	24.0	0.0000
CiteSeer	365154	9.4	1739	4.1	-0.0632	15	1850	25.4	0.3787
Zhishi	372840	12.4	127066	2243.5	-0.2825	228	449	282.7	0.0582
Actor coll. net	374511	80.2	3956	4.2	0.2260	365	1178	553.7	0.0753
Amazon, Mar.12,2003	400727	11.7	2747	1.6	-0.0203	10	27046	13.3	0.3788
Amazon, Jun.6,2003	403364	12.1	2752	1.5	-0.0176	10	32886	13.4	0.4025
Amazon, May5,2003	410236	11.9	2760	1.6	-0.0169	10	32632	13.4	0.4177
Petster, dogs	426485	40.1	46503	50.3	-0.0884	248	1177	386.6	0.1198
Road network PA	1087562	2.8	9	0.1	0.1220	3	916	3.3	0.0208
YouTube friend. net.	1134890	5.3	28754	92.9	-0.0369	51	845	86.1	0.2458
Road network TX	1351137	2.8	12	0.1	0.1271	3	1491	3.4	0.0495
AS Skitter	1694616	13.1	35455	109.4	-0.0814	111	222	150.0	0.0451
Road network CA	1957027	2.8	12	0.1	0.1206	3	4454	3.3	0.0268
Wikipedia, pages	2070367	40.9	230040	80.8	-0.0418	208	702	283.4	0.0895
US Patents	3764117	8.8	793	1.4	0.1675	64	106	76.3	0.0079
DBpedia	3915921	6.4	469692	2156.2	-0.0427	20	70	27.9	0.0620
LiveJournal	5189808	18.8	15016	7.3	0.0394	374	415	408.9	0.0006

TABLE I: Topological properties of the real networks considered: Network size  $N$ ; average degree  $\langle q \rangle$ ; maximum degree  $q_{\max}$ ; heterogeneity parameter  $\chi = \langle q^2 \rangle / \langle q \rangle^2 - 1$ ; degree correlations as measured by the Pearson coefficient  $r$  [36]; maximum core index  $K_M$ ; size of the maximum core  $N_{K_M}$ ; average internal degree of the maximum core  $\langle q \rangle_{K_M}$ ; heterogeneity parameter of the maximum core  $\chi_{K_M} = \langle q^2 \rangle_{K_M} / \langle q \rangle_{K_M}^2 - 1$ .



- 
- [1] P. Van Mieghem, *Graph Spectra for Complex Networks* (Cambridge University Press, Cambridge, U.K., 2011).
- [2] A. N. Samukhin, S. N. Dorogovtsev, and J. F. F. Mendes, “Laplacian spectra of, and random walks on, complex networks: Are scale-free architectures really important?” *Phys. Rev. E* **77**, 036115 (2008).
- [3] Santo Fortunato, “Community detection in graphs,” *Physics Reports* **486**, 75–174 (2010).
- [4] Brian Karrer, M. E. J. Newman, and Lenka Zdeborová, “Percolation on sparse networks,” *Phys. Rev. Lett.* **113**, 208702 (2014).
- [5] Mark Newman, *Networks: An Introduction* (Oxford University Press, Inc., New York, NY, USA, 2010).
- [6] Phillip Bonacich, “Factoring and weighting approaches to status scores and clique identification,” *Journal of Mathematical Sociology* **2**, 113–120 (1972).
- [7] D. Chakrabarti, Y. Wang, C. Wang, J. Leskovec, and C. Faloutsos, “Epidemic thresholds in real networks,” *ACM Trans. Inform. Syst. Sec.* **10**, 13 (2008).
- [8] Juan G. Restrepo, Edward Ott, and Brian R. Hunt, “Onset of synchronization in large networks of coupled oscillators,” *Phys. Rev. E* **71**, 036151 (2005).
- [9] Juan G. Restrepo, Edward Ott, and Brian R. Hunt, “Weighted percolation on directed networks,” *Phys. Rev. Lett.* **100**, 058701 (2008).
- [10] Andrew Pomerance, Edward Ott, Michelle Girvan, and Wolfgang Losert, “The effect of network topology on the stability of discrete state models of genetic control,” *Proceedings of the National Academy of Sciences* **106**, 8209–8214 (2009).
- [11] Osame Kinouchi and Mauro Copelli, “Optimal dynamical range of excitable networks at criticality,” *Nat Phys* **2**, 348–351 (2006).
- [12] S N Dorogovtsev, A V Goltsev, J F F Mendes, and A N Samukhin, “Spectra of complex networks,” *Phys. Rev. E* **68**, 046109 (2003), arXiv:0306340 [cond-mat].
- [13] Dong-Hee Kim and Adilson E. Motter, “Ensemble Averageability in Network Spectra,” *Phys. Rev. Lett.* **98**, 248701 (2007).
- [14] Raj Rao Nadakuditi and M. Newman, “Spectra of random graphs with arbitrary expected degrees,” *Phys. Rev. E* **87**, 012803 (2013).
- [15] J. G. Restrepo, E. Ott, and B. R. Hunt, “Approximating the largest eigenvalue of network adjacency matrices,” *Phys. Rev. E* **76**, 056119 (2007).
- [16] Albert-László Barabási and R. Albert, “Emergence of scaling in random networks,” *Science* **286**, 509–512 (1999).
- [17] F. Chung, L. Lu, and V. Vu, “Spectra of random graphs with given expected degrees,” *Proc. Natl. Acad. Sci. USA* **100**, 6313–6318 (2003).
- [18] M. Boguñá, R. Pastor-Satorras, and A. Vespignani, “Cut-offs and finite size effects in scale-free networks,” *Euro. Phys. J. B* **38**, 205–210 (2004).
- [19] M. Boguñá and R. Pastor-Satorras, “Class of correlated random networks with hidden variables,” *Phys. Rev. E* **68**, 036112 (2003).
- [20] Fan Chung, Linyuan Lu, and Van Vu, “Eigenvalues of Random Power law Graphs,” *Ann. Comb.* **7**, 21–33 (2003).
- [21] S. N. Dorogovtsev and J. F. F. Mendes, “Evolution of networks,” *Advances in Physics* **51**, 1079–1187 (2002).
- [22] Claudio Castellano and Romualdo Pastor-Satorras, “Thresholds for epidemic spreading in networks,” *Phys. Rev. Lett.* **105**, 218701 (2010).
- [23] Gene H Golub and Charles F Van Loan, *Matrix computations*, Vol. 3 (JHU Press, Baltimore, 2012).
- [24] M. Catanzaro, M. Boguñá, and R. Pastor-Satorras, “Generation of uncorrelated random scale-free networks,” *Phys. Rev. E* **71**, 027103 (2005).
- [25] Filippo Radicchi and Claudio Castellano, “Breaking of the site-bond percolation universality in networks,” *Nature communications* **6**, 10196 (2015).
- [26] Claudio Castellano and Romualdo Pastor-Satorras, “Competing activation mechanisms in epidemics on networks,” *Scientific Reports* **2**, 00371 (2012).
- [27] Romualdo Pastor-Satorras and Claudio Castellano, “Distinct types of eigenvector localization in networks,” *Sci. Rep.* **6**, 18847 (2016).
- [28] Stephen B. Seidman, “Network structure and minimum degree,” *Social Networks* **5**, 269–287 (1983).
- [29] S. N. Dorogovtsev, A. V. Goltsev, and J. F. F. Mendes, “k-core organization of complex networks,” *Phys. Rev. Lett.* **96**, 040601 (2006).
- [30] A. V. Goltsev, S. N. Dorogovtsev, J. G. Oliveira, and J. F. F. Mendes, “Localization and Spreading of Diseases in Complex Networks,” *Phys. Rev. Lett.* **109**, 128702 (2012).
- [31] T. Martin, X. Zhang, and M. E. J. Newman, “Localization and centrality in networks,” *Phys. Rev. E* **90**, 052808 (2014).
- [32] Shankar Bhamidi, Steven N. Evans, and Arnab Sen, “Spectra of large random trees,” *Journal of Theoretical Probability* **25**, 613–654 (2012).
- [33] M. Krivelevich and B. Sudakov, “The largest eigenvalue of sparse random graphs,” *Combinatorics, Probability and Computing* **12**, 61–72 (2003).
- [34] S. N. Dorogovtsev, J. F. F. Mendes, and A. N. Samukhin, “Structure of Growing Networks with Preferential Linking,” *Physical Review Letters* **85**, 4633–4636 (2000).
- [35] Alain Barrat and Romualdo Pastor-Satorras, “Rate equation approach for correlations in growing network models,” *Physical Review E* **71**, 036127 (2005).
- [36] M. E. J. Newman, “Assortative mixing in networks,” *Phys. Rev. Lett.* **89**, 208701 (2002).
- [37] R. Pastor-Satorras, A. Vázquez, and A. Vespignani, “Dynamical and correlation properties of the Internet,” *Phys. Rev. Lett.* **87**, 258701 (2001).
- [38] Abraham Flaxman, Alan Frieze, and Trevor Fenner, “High Degree Vertices and Eigenvalues in the Preferential Attachment Graph,” *Internet Mathematics* **2**, 1–19 (2005).
- [39] S. Maslov and K. Sneppen, “Specificity and stability in topology of protein networks,” *Science* **296**, 910–913 (2002).
- [40] Daniel B. Larremore, Woodrow L. Shew, and Juan G. Restrepo, “Predicting criticality and dynamic range in complex networks: Effects of topology,” *Phys. Rev. Lett.* **106**, 058101 (2011).
- [41] R. M. Anderson and R. M. May, *Infectious diseases in humans* (Oxford University Press, Oxford, 1992).
- [42] R. Pastor-Satorras and A. Vespignani, “Epidemic spreading in scale-free networks,” *Phys. Rev. Lett.* **86**, 3200–3203 (2001).

- [43] Juan A. Acebrón, L. L. Bonilla, Conrad J. Pérez Vicente, Félix Ritort, and Renato Spigler, “The Kuramoto model: A simple paradigm for synchronization phenomena,” *Rev. Mod. Phys.* **77**, 137–185 (2005).
- [44] Alex Arenas, Albert Díaz-Guilera, Jurgen Kurths, Yamir Moreno, and Changsong Zhou, “Synchronization in complex networks,” *Physics Reports* **469**, 93 – 153 (2008).
- [45] Francisco A. Rodrigues, Thomas K. DM. Peron, Peng Ji, and Jürgen Kurths, “The Kuramoto model in complex networks,” *Phys. Rep.* **610**, 1–98 (2016).
- [46] Notice that in many cases the hub actually is part of the maximum  $K$ -core. Nevertheless there is a clear distinction between the case the PEV is localized on the hub and its immediate neighbors or the PEV is localized around the maximum  $K$ -core as a whole.
- [47] Leo Katz, “A new status index derived from sociometric analysis,” *Psychometrika* **18**, 39–43 (1953).
- [48] D. J. de Solla Price, “A general theory of bibliometric and other cumulative advantage processes,” *J. Amer. Soc. Inform. Sci.* **27**, 292 (1976).
- [49] M. Boguñá, C. Castellano, and R. Pastor-Satorras, “Langevin approach for the dynamics of the contact process on annealed scale-free networks,” *Phys. Rev. E* **79**, 036110 (2009).
- [50] M.J. Keeling and P. Rohani, *Modeling Infectious Diseases in Humans and Animals* (Princeton University Press, 2007).
- [51] Romualdo Pastor-Satorras, Claudio Castellano, Piet Van Mieghem, and Alessandro Vespignani, “Epidemic processes in complex networks,” *Rev. Mod. Phys.* **87**, 925–979 (2015).
- [52] Romualdo Pastor-Satorras and Alessandro Vespignani, “Epidemic dynamics and endemic states in complex networks,” *Phys. Rev. E* **63**, 066117 (2001).
- [53] S. N. Dorogovtsev, A. V. Goltsev, and J. F. F. Mendes, “Critical phenomena in complex networks,” *Rev. Mod. Phys.* **80**, 1275–1335 (2008).
- [54] Silvio C. Ferreira, Claudio Castellano, and Romualdo Pastor-Satorras, “Epidemic thresholds of the susceptible-infected-susceptible model on networks: A comparison of numerical and theoretical results,” *Phys. Rev. E* **86**, 041125 (2012).
- [55] Marian Boguñá, Claudio Castellano, and Romualdo Pastor-Satorras, “Nature of the epidemic threshold for the susceptible-infected-susceptible dynamics in networks,” *Phys. Rev. Lett.* **111**, 068701 (2013).
- [56] Angélica S. Mata, Marian Boguñá, Claudio Castellano, and Romualdo Pastor-Satorras, “Lifespan method as a tool to study criticality in absorbing-state phase transitions,” *Phys. Rev. E* **91**, 052117 (2015).